COUPLED INDUCTOR RESONANT SWITCHED CAPACITOR VOLTAGE EQUALIZER FOR PHOTOVOLTAIC PARTIAL SHADING COMPENSATION

Cláudio H. G. dos Santos[1], Pedro F. Donoso-Garcia[2], Seleme I. Seleme Junior[3]
[1]Federal Center of Technological Education of Minas Gerais, Divinópolis – MG, Brazil
[2, 3] Federal University of Minas Gerais, Belo Horizonte – MG, Brazil
[1]claudiosantos@cefetmg.br, [2]pedro@cpdee.ufmg.br, [3]seleme@cpdee.ufmg.br

***Abstract* – Switched capacitor converters play an important role in various applications in power electronics. Voltage equalizers are one of them, and have been applied for partial shading compensation in photovoltaic systems. In other works, the switched capacitor, have been improved with the addition of a small inductor, becoming a resonant converter with many advantages compared to switched capacitor. However, this converter can still be improved in many aspects, rather in its effective resistance, equalized voltage drop, and current stress. In this paper, a novel Coupled Inductor Resonant Switched Capacitor voltage equalizer is proposed. The comparison between all circuits here studied is developed through simulation results. Also, the proposed circuit experiment results are presented. At the end, conclusions summing the paper contribution are made.**

***Keywords* – Switched Capactior Converter, Resonant Switched Capacitor, Coupled Inductors, Partial shading, Voltage Equalizers.**

NOMENCLATURE

V_{PVn}	Voltage of the index module n
I_{PVn}	Current of the index module n
C_{dn}	PV module index n capacitor
R_n	ESR index n capacitor
R_{swn}	Switch n index on resistance
V_{PVn}	Voltage of the index module n
C_{dn}	PV module index n capacitor
R_x	ESR of switched capacitor
R_{xn}	ESR index n resonant capacitor
R_L	Load resistance
L_x	Inductance of resonant capacitor
L_{xn}	Leakage inductance of index n
L_m	Mutual inductance of coupled inductors

I. INTRODUCTION

Photovoltaic (PV) energy is each day more common and accessible for consumers in general. This growth is strongly dependent on cost and feedback, since the project is an investment. To keep growing in number and quality, researchers and industries has focused in the grid inverter and PV modules enhancements, and hence, in the last years, the number of manufacturers of has increased more than in many decades before [1]. The solutions became more cheap and accessible, and PV modules had its efficiency and peak power increase significantly. However, that are still problems that manufacturers do not address it.

In [2] is presented an extended study about mismatch conditions and its unstable closed loop relation with degradation mechanisms. There are many types of mismatch conditions, e.g., partial shading, temperatures difference and soil. All module are susceptible to it, whether is naturally induced. Mismatch conditions manifest in differences between voltages and currents between modules installed in the same array. Degradation mechanisms are permanent damage in PV modules caused by mismatch conditions and that aggravates even more this conditions. In sum, this process occurs in PV modules array, and due to presence of mismatch, may last less than expected, presenting accelerated aging. The most common mismatch condition is the partial shading, that reduces the current of shaded modules [3]. As consequence, these modules tends to be bypassed by diodes, being discarded from its string, and thus, presenting multiple maximum power point (MPP), what interfere with the maximum power point tracker algorithm.

As solution, integrated converters can be applied to enable PV modules to operate with current mismatch. Thus, each module is able to deliver its maximum power. Among the many types of integrated converters, Voltage Equalizers (VE) present an efficiency solution, since can be turn off when partial shading is not present. In this way, only part of the power is processed, therefore, being denominated as Partial Power Converter [4]. The microinverter is also a suitable solution, however, as a full power converter, it submits all PV power to a lower efficiency when partial shading is not present.

Fig. 1 (a) and (b), show IxV and PxV characteristic curves, respectively. The red curve represents a string with bypass diodes, and blue curve represents the output of string in which a voltage equalizer is operating. Both systems are affected with the same partial shading profile, or same mismatch. As can be observed, the voltage equalizer extract all power available, not discarding the shaded module as the diode bypass does, [5].

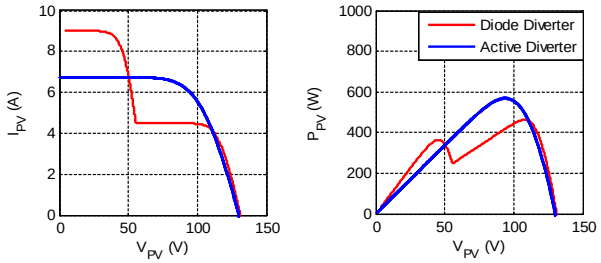

Fig. 1. Diode bypass diverter and voltage equalizers comparison: (a) IxV curve comparison; (b) PxV curve comparison.

Voltage equalizers circuits may appears in many types of architectures and topologies. In [6], a comparative analysis of a variety of this circuit is presented. Among all circuits approached, the Switched Capacitor is a very suitable solution, and can be applied to strings of any number of PV modules. A better version of the SC is introduced and detailed in [7]–[11]. Known as Resonant Switched Capacitor (ReSC), it brings many advantages like easier implementation, zero current switching that enables increase the converter frequency without affecting its efficiency, [12].

Fig.2 (a), (b) and (c) illustrates the Switched Capacitor (SC) Voltage Equalizer (VE) for two, three and four modules string, respectively. The shaded modules are grey and the full radiated module are white. As noticed, the converter consists of one Half Bridge (HB) connected to each module and with the output connected to the adjacent HB output through a capacitor. When switching at a proper frequency with fixed 50% duty cycle, the modules voltages are equalized no matter the irradiance mismatch, requiring no cloed loop operation. Therefore, all modules may operate with different current, and deliver its total power.

The SC converters are known as an option to avoid use magnetic components [12], i.e. large core inductors needed to work as current filters. This enable circuits to operate with higher frequency without increasing losses. In [13], a circuit similar of those shown in Fig. 2 are used as transformerless step-up converters, with efficiency reaching levels above 95%. In [14], a bridgeless boost rectifier is developed using SC concept. Also, its maximum efficiency is above 95% a. In [15], an on-grid inverter based on SC presents considerably high performance and efficiency. In [16], a high gain SC boost converter is developed based in SC, reaching gains from 2 to 16 times the input, also with high efficiency.

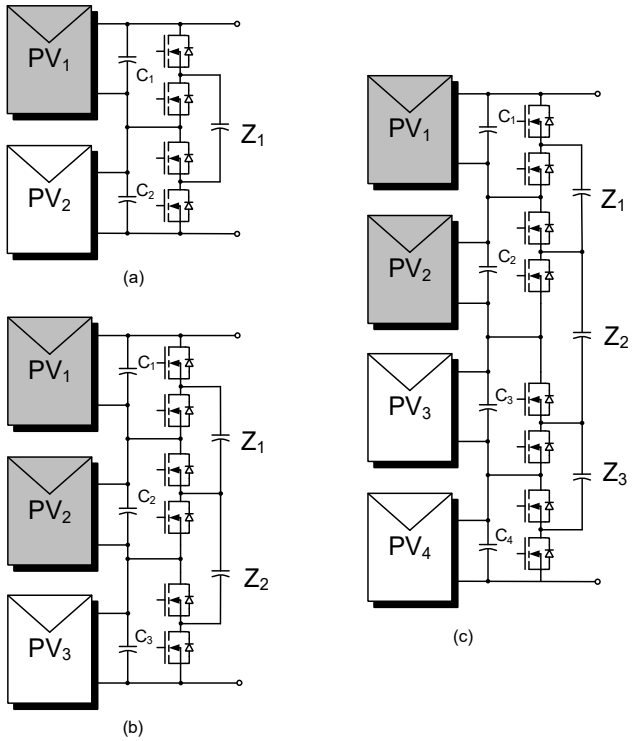

Fig. 2. Switched Capacitors voltage equalizers: (a) SC for two modules string; (b) SC for three modules string; (c) SC for four modules string.

In this paper, a new voltage equalizer circuit is proposed, based o ReSC and applying coupled inductor to enhance its performance. Next section, the SC VE is modeled and its waveforms are detailed. In this model, is established a relation between mismatch and equalized voltage drop, also valid for ReSC. In section 3, the ReSC is detailed and compared with the SC, showing how resonance can improve a converter. In section 4, the proposed circuit, here denominated Coupled Inductor Resonant Switched Capacitor (CI-ReSC) is presented. In section 5, simulation results of SC, ReSC and CI-ReSC are shown. In section 6, experimental results are provided to support theoretical development. At the final section, conclusions are made.

II. THE SWITCHED CAPACITOR VOLTAGE EQUALIZER

To better understand ReSC and the proposed CI-ReSC, in this section, the SC is explained in detail, and a State Average model is developed to put in analytical form the Equalized Voltage Drop (EVD), and the Switched Capacitor Current (I_{SC}). This analysis will serve as guideline for designing this voltage equalizer based on PV modules parameters. It should be clarified that, the EVD is the voltage difference between the modules when the VE is operating.

Fig. 3 (a) and (b) the SC switching modes are shown. In Fig. 3 (a), the capacitor C_x is connected to PV_1 and in Fig. 3 (b) is connected to PV_2. In this circuit, it can be observed that the capacitor model considers its Equivalent Series Resistance (ESR), henceforth denoted as R_X. In Fig. 3 (c) waveform are illustrated, in which the first two signals are the commands for upper and down switch of both bridges. The third waveform represents the voltage applied on the capacitor. This voltage has a square waveform with offset value equal to the PV_1 and PV_2 voltages arithmetic average. Also, the capacitor voltage is denoted as V_C, and with proper frequency will operate as a filter. The last waveform represents capacitor current I_C, whose peak value is equal to the difference between PV_1 and PV_2 modules.

It should be clarified that, when switching with frequencies many times higher than the natural frequency of R_X and C_X, I_C will have a square waveform, and V_C will have triangular waveform.

For design guidelines, it is necessary to calculate I_C, which depends on V_C, R_X and switching frequency (f_{sw}). To calculate V_C, the circuit can modeled in average state space, in which the V_{PV1}, V_{PV2} and V_C are the states.

Fig. 4 (a) and (b) illustrates the two circuits that result of switching and that for, can be used as system A_1 and A_2, respectively. In this circuits, the mismatched modules are represented by ideal current sources I_{PV1} and I_{PV2}. The capacitor C_1 and C_2 are connected to the modules, and its ESR are, respectively, R_1 and R_2. The resistances R_{SW1}, R_{SW2}, R_{SW3} and R_{SW4} represents all four switches on resistance. The switched capacitor is represented by C_X and its ESR R_X. The resistance R_L represents the circuit load.

Average state space is a method commonly used to model converters based on their parameter and switching, [17]. The method consists in determining one system for each switching mode, as demonstrated in eq. (1), as following,

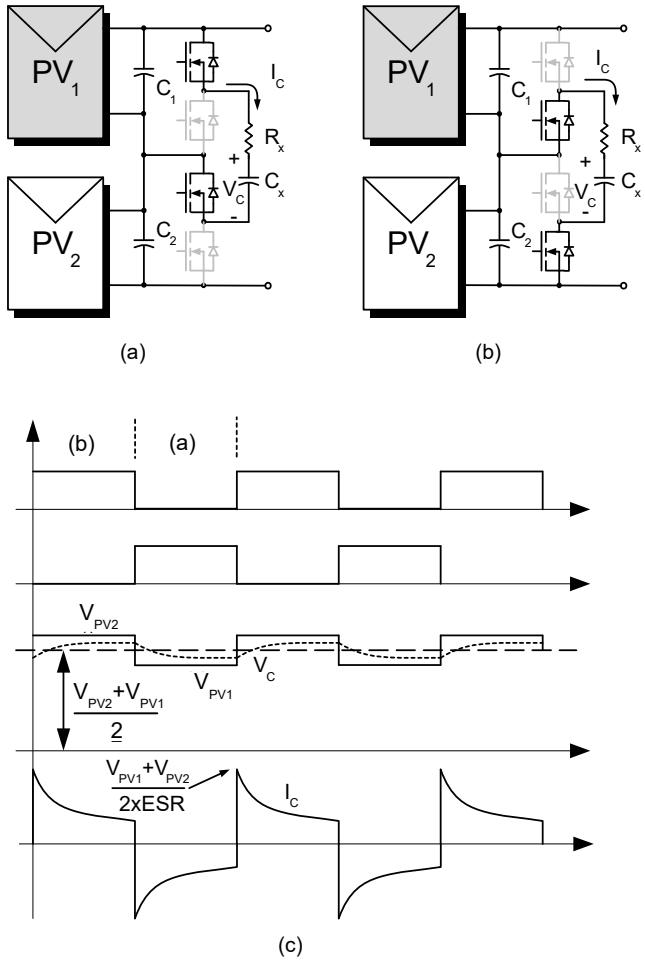

Fig. 3. Switched Capacitor Voltage Equalizer circuit and waveforms: (a) PV_1 connected to SC; (b) PV_2 connected to SC; (c) Voltage and Current waveform.

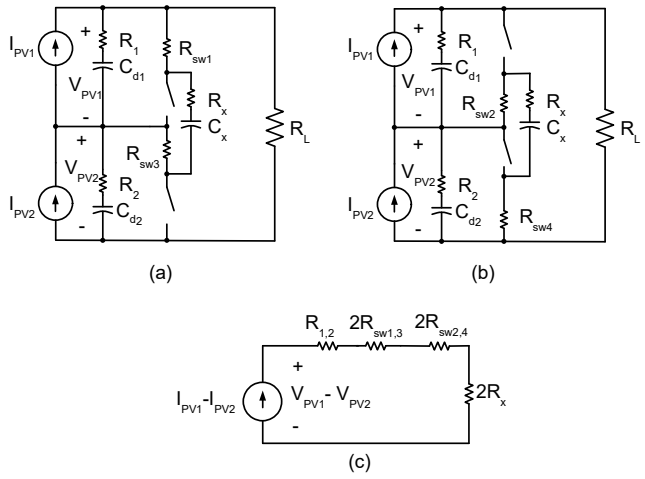

Fig. 4. SC Switching modes for average state space modeling: (a) system A1; (b) system A2; (c) equivalent circuit.

$$
\begin{aligned}
\mathbf{A} &= A_1 D + A_2 (1-D) \\
\mathbf{B} &= B_1 D + B_2 (1-D) \\
\mathbf{C} &= C_1 D + C_2 (1-D) \\
\mathbf{D} &= D_1 D + D_2 (1-D) \\
\dot{X} &= \mathbf{A}X + \mathbf{B}U = 0 \\
Y &= \mathbf{C}X + \mathbf{D}U
\end{aligned} \tag{1}
$$

where, matrix **A** is the full model, A_1 and A_2 are the models illustrated in Fig. 4 (a) and (b), respectively. The same goes to **B**, **C** and **D** matrices.

Applying average state space, the models for each switching mode can be obtained in eqs. (2) and (3) as following,

$$
\begin{bmatrix} \dot{v}_{PV1} \\ \dot{v}_{PV2} \\ \dot{v}_C \end{bmatrix} = \begin{bmatrix} \frac{1}{C_x}\left(\frac{1}{R_L} + \frac{1}{R_{sw1}+R_{sw3}+R_x}\right) & \frac{-1}{R_L C_{d1}} & \frac{1}{(R_{sw1}+R_{sw3}+R_x)C_{d1}} \\ \frac{-1}{R_L C_{d2}} & \frac{-1}{R_L C_{d2}} & 0 \\ \frac{1}{(R_{sw1}+R_{sw3}+R_x)C_x} & 0 & \frac{-1}{(R_{sw1}+R_{sw3}+R_x)C_x} \end{bmatrix} \times \ldots
$$

$$
\ldots \begin{bmatrix} v_{PV1} \\ v_{PV1} \\ v_C \end{bmatrix} + \begin{bmatrix} \frac{1}{C_{d1}} & 0 \\ 0 & \frac{1}{C_{d2}} \\ 0 & 0 \end{bmatrix} \begin{bmatrix} i_{PV1} \\ i_{PV2} \end{bmatrix} \tag{2}
$$

$$
y = [1 \quad -1 \quad 0] \begin{bmatrix} v_{PV1} \\ v_{PV2} \\ v_C \end{bmatrix}
$$

$$
\begin{bmatrix} \dot{v}_{PV1} \\ \dot{v}_{PV2} \\ \dot{v}_C \end{bmatrix} = \begin{bmatrix} \frac{1}{C_x}\left(\frac{1}{R_L} + \frac{1}{R_{sw1}+R_{sw3}+R_x}\right) & \frac{-1}{R_L C_1} & \frac{1}{(R_{sw1}+R_{sw3}+R_x)C_1} \\ \frac{-1}{R_L C_2} & \frac{-1}{R_L C_2} & 0 \\ \frac{1}{(R_{sw1}+R_{sw3}+R_x)C_x} & 0 & \frac{-1}{(R_{sw1}+R_{sw3}+R_x)C_x} \end{bmatrix} \times \ldots
$$

$$
\ldots \begin{bmatrix} v_{PV1} \\ v_{PV2} \\ v_C \end{bmatrix} + \begin{bmatrix} \frac{1}{C_1} & 0 \\ 0 & \frac{1}{C_2} \\ 0 & 0 \end{bmatrix} \begin{bmatrix} i_{PV1} \\ i_{PV2} \end{bmatrix} \tag{3}
$$

$$
y = [1 \quad -1 \quad 0] \begin{bmatrix} v_{PV1} \\ v_{PV2} \\ v_C \end{bmatrix}
$$

Applying eqs. (2) and (3) in eq. (1), and considering non state variation, the solution of this linear system leads to eq. (4), as following,

$$
V_{PV1} - V_{PV2} = 2\left(R_x + R_{sw1,3} + R_{sw2,4}\right)\left(I_{PV1} - I_{PV2}\right) \tag{4}
$$

indicating that EVD (V_{PV1}-V_{PV2}) is dependent on the current mismatch and all the other elements resistance

The switched capacitor peak current $I_{C,pk}$ can be calculated by eq. (5), using the EVD in eq. 4 divided by the total circuit resistance.

$$
I_{pk} = \frac{V_{PV1} - V_{PV2}}{2\left(R_x + R_{sw1,3} + R_{sw2,4}\right)}\left(2 - e^{1/2\left(R_x + R_{sw1,3} + R_{sw2,4}\right)C_x f_{sw}}\right) \tag{5}
$$

Considering all switches with same resistance R_{sw}, and switching with considerably higher frequency than the circuit natural frequency, the capacitor current will assume a square waveform, which peak can be calculated simply through eq. (6), as following,

$$I_{pk} = \frac{V_{PV1} - V_{PV2}}{2\left(R_x + 2R_{sw}\right)} \quad (6)$$

With this available data, the guidelines for design the circuit can be stated. The SC VE is a valid option to compensate the partial shading, however, as will be discussed in next section and demonstrated in simulation results, it is more valid to implement ReSC, due to various advantages.

III. THE RESONANT SWITCHED CAPACITOR VOLTAGE EQUALIZER

The ReSC is an enhanced version of the SC circuit, in which a small inductor is connected in series with the switched capacitor. In this circuit, both inductor and capacitor constitutes resonant circuit. The circuit is designed to switch on the resonant frequency. Thus, brings a series of advantages, including quasi zero current switching, allowing use of smaller switched capacitor, and reducing stress on switching.

Fig. 5 illustrates the basic difference between this two voltage equalizers. Fig. 5 (a) and (b) show the SC and the ReSC for a two module mismatched string, and Fig. 5 (c) and (d), show their frequency response, respectively. Note that in both frequency response, the switching frequency and natural circuit frequency are highlighted. In SC, the switching frequency must be several times the natural frequency, while in ReSC their must be the same. It means that, for the same switching frequency the ReSC capacitance, will be several times smaller. Also, another advantage is that, the ReSC natural frequency is determined by L_x and C_x, instead of R_x and C_x, in the SC. This gives the designer, the control over the natural frequency, since R_x is an intrinsic not purposeful capacitor parameter.

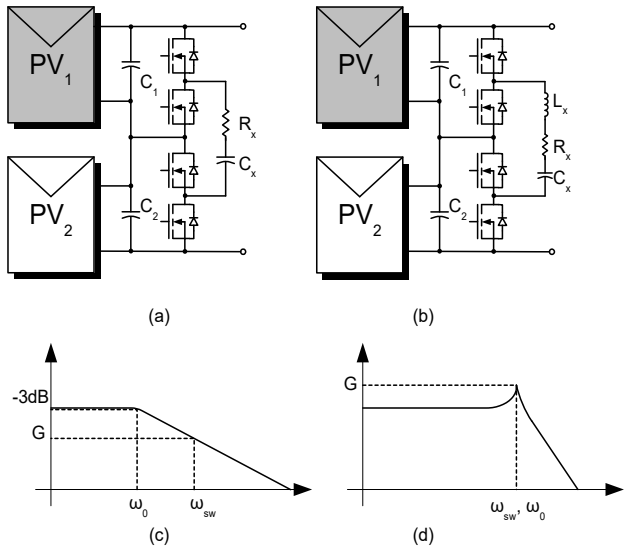

Fig. 5. SC and ReSC filter response omparison.

Fig. 6 illustrates the ReSC switching modes operation, similar to the SC. First two graphs show the switching commands for the bridges. The third gurve shows the voltage over the entire resonant impedance, together with the C_x voltage, which is sinusoidal, as the capacitor current I_C.

Although the ReSC brings many benefits compared with SC, the compensated voltage difference and its capacitor current peak will, have, practically, the same values of the SC, as will be shown through simulation results in section V. The inductor addition in the ReSC does not affect the overall resistance. Thus the equations (4) and (6) can be also be used in the converter design.

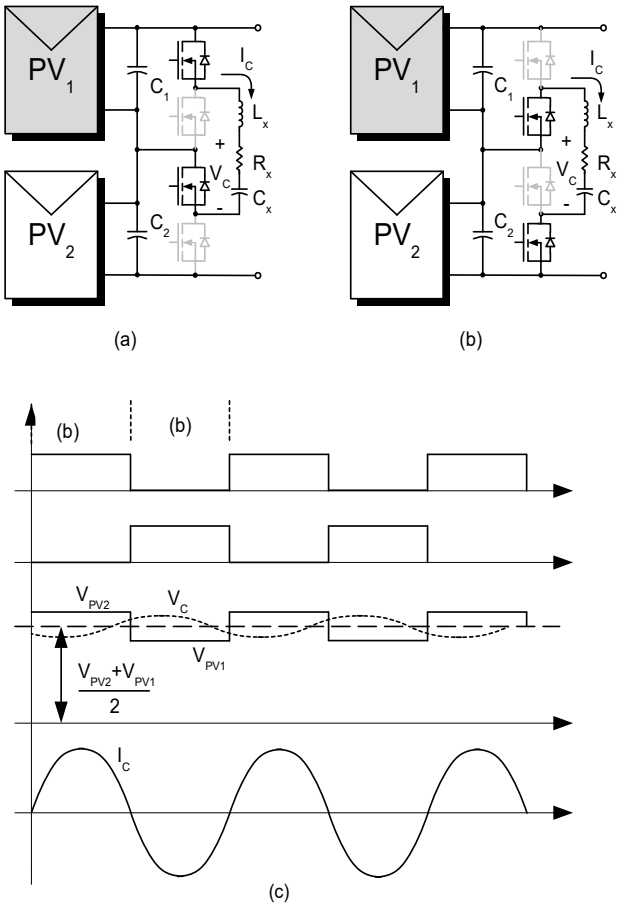

Fig. 6. Resonant Switched Capacitor Voltage Equalizer circuit: (a) PV1 connected to ReSC; (b) PV2 connected to ReSC; (c) Voltage and current waveform.

IV. PROPOSED COUPLED INDUCTOR RESONANT SWITCHED CAPACITOR VOLTAGE EQUALIZER

In this section, we develop the CI-ReSC, shown in Fig. 7. This circuit is introduced in [18], and its a result of a study about various types of voltage equalizers of different architectures and topologies. The basic idea is two double the circuit bridges and use a coupled inductor connected between the bridges. The dispersion of this inductors, L_{X1} and L_{X2} will replace the role of L_X in the ReSC. Therefore, with the bridges switching 180° phase-shift, the magnetic flux generated by each current will be canceled. Also, the ripple produced by each bridge will be significant smaller, since many components will be canceled by the phase shift.

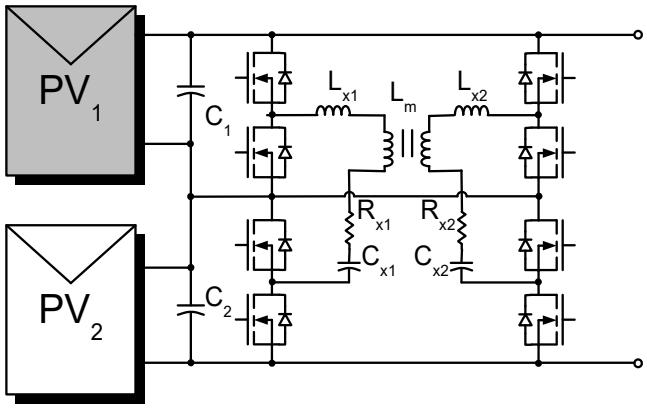

Fig. 7. Proposed Coupled Inductor Resonant Switched Capacitor voltage equalizer.

With smaller currents, the EVD will be significantly reduced, allowing the choice of even smaller capacitors. It is also important to mention that, although the number of components are doubled, their current stress will be highly reduced as also their losses and sizing features.

Although in [7]–[11], a coreless inductor is used to implement L_X, for the CI-ReSC a ferrite core is used for better coupling. It should be also clarified that, the natural frequency for this circuit will formed by $L_{X1}C_1$ and $L_{X2}C_2$ and the magnetizing inductance will not affect the circuit operation, due to the current cancellation caused by the 180° phase shift between the HB switching.

Fig. 8 (a) and (b) show the switching modes for the CI-ReSC considering current sources with different currents as the mismatched PV modules. As done in section II, the average state space for the CI-ReSC was developed considering modes A_1 and A_2 in Fig. 8 (a) and (b), respectively, resulting, however, in a non-minimal system. An attempt to model the ReSC circuit using average state space was made, also resulting in a non-minimal system. Therefore, to model the CI-ReSC in order provide a method of sizing it, is proposed its equivalent AC model.

Fig. 8 (c) shows the CI-ReSC AC model. As can be noticed, the resonant circuits branches are connected to two different current sources. The current sources are 180° phase shifted and its amplitude equals half the current difference between modules. Considering each branch a band pass filter with its natural frequency equals the current source switching frequency, it is clear that the fundamental component will be majorly present. The other frequencies will have minor gain, and thus, can de neglected.

By analyzing the circuit in Fig. 8 (c) considering only the fundamental frequency, the phasor analysis indicates that only the resistances will be considered in the voltage drop of each branch. This is because $L_{x1,2}$ and $C_{x1,2}$ voltage drops cancel each other in this exact frequency. About the mutual inductance L_m, its voltage drop is also canceled by the two 180° phase shifted currents.

Thus the EVD in this circuit can be expressed by eq. (7), which is half the EVD of ReSC and SC. The current peak in each branch can be represented by eq. 8.

$$V_{PV1} - V_{PV2} = \left(R_x + 2R_{sw}\right)\left(I_{PV1} - I_{PV2}\right) \qquad (7)$$

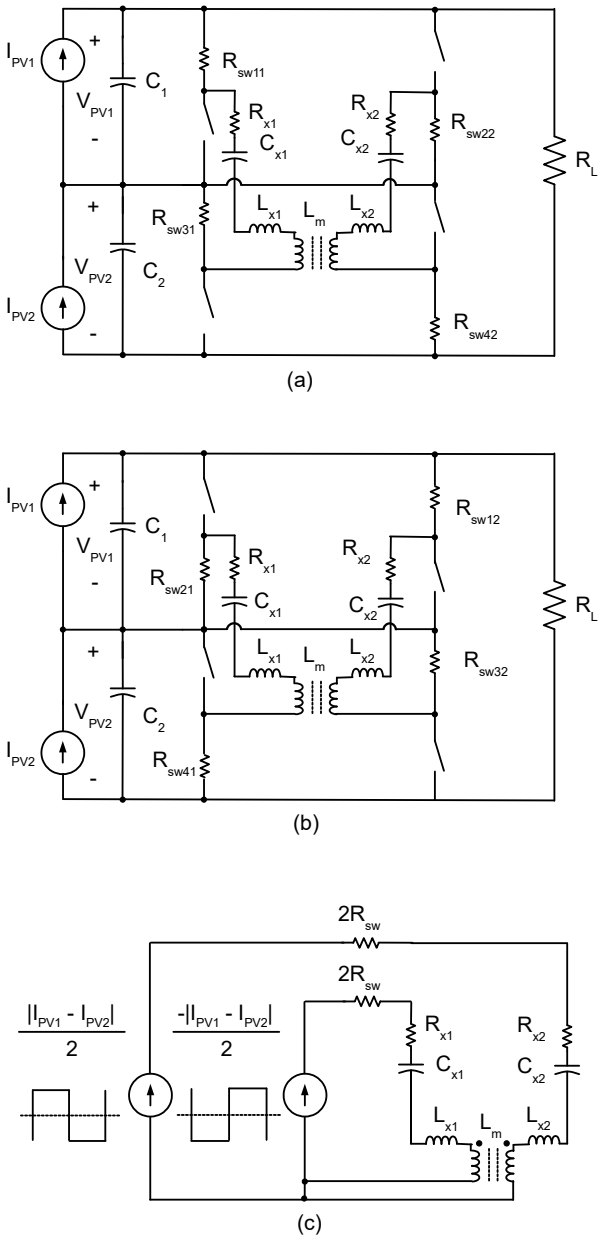

Fig. 8. - CI-ReSC Switching modes for modeling: (a) Switches 11, 31, 22 and 42 closed; (b) Switches 21, 41, 12 and 32 closed; (c) AC equivalent circuit.

About the current, since each branch have half the current deviated, the same partial power will processed by the CI-ReSC. However, due to the 180° phase shift and consequently the current cancellation between the resonant branch currents, the drained current from the PV module capacitors will decrease significantly compared to ReSC and SC converter. Therefore, it can be chosen considerably smaller C_{d1} and C_{d2} capacitors to achieve the same voltage ripple in the modules. In sum, although more component are necessary, there dimensions are reduced compared to ReSc and SC.

V. SIMULATION RESULTS

In this section, SC, ReSC and CI-ReSC PSIM® simulation results are shown, analyzed and discussed. In Table I, simulation parameters for all these three circuits are shown. The comparison criteria is the capacitor current, the voltage ripple and equalized voltage drop. The same parameters are used in all circuit simulations, except the switched capacitor C_X. For SC voltage equalizer, the capacitance must be several times higher than ReSC and CI-ReSC, since it operates far beyond its natural frequency.

Table 1 – Simulation Parameters.

Parameters	Value
Switching Frequency – f_{sw}	100 kHz
60 Cell PV Module – I_{SC}	9 A
60 Cell PV Module – V_{OC}	36 V
60 Cell PV Module – P_{max}	250 W
Module Capacitor – C_1, C_2	22µF
SC – C_X	350µF
ReSC – C_X	22µF
CI-ReSC – C_X	22µF
Inductor – L_X, L_{X1} and L_{X2}	115nH
Equivalent Series Resistance – R_X	44mOhm
Magnetizing Inductance – L_m	7.7µH

Fig. 10 shows a comparison between capacitor current I_C for both SC and ReSC voltage equalizers. As can be noticed, the SC capacitor is as expected, following an exponential decay that is changed in initial state every cycle. Also, as expected, the ReSC capacitor current is sinusoidal and has the same peak as the SC, since both current depends on the overall circuit resistance form the capacitor viewpoint. As will be further discussed, the main benefit of sinusoidal current waveform is switching stress.

Fig. 11 shows the modules voltages for both SC and ReSC voltage equalizer. As can be observed, both voltage equalizers presents similar results, with approximate voltage ripple and equalized voltage drop. In this case, the SC presents smaller EVD and voltage ripple.

Fig. 12 shows switch voltages and currents for both SC and ReSC. This results show that for both turn off and turn on transients, the SC has high levels of current, resulting switching losses, and hence is less efficient, while in the ReSC, the switch current is almost zero. This feature, will not only be a benefit for efficient, but also for electromagnetic compatibility of the entire system. Since MOSFET or faster switches must be used, and since it operates with high frequency, way above the on grid inverter switching frequencies, a fast transition current of SC would much likely generate electromagnetic interference (EMI) than the sinusoidal current from ReSC.

It is clear that ReSC has advantages compared SC, mainly regarding component sizing. As can be observed, the SC switched capacitor has to be 350 µF, a high value for this application, while the ReSC needs only 22 µF.

Fig. 13 shows simulation results comparing both ReSC and CI-ReSC. In Fig. 11 (a), module voltages are compared, and as can be noticed, CI-ReSC presents, approximately, half the ripple and the EVD by ReSC. Also, the ripple for CI-ReSC has double the frequency compared to ReSC, which allows the choice of smaller module capacitors. Another advantage, is that, since EVD is smaller, both modules will operate near the same MPP than the ReSC, since voltage are better equalized.

Fig. 11 (b), shows capacitor current for circuits, and also, as expected, the CI-ReSC capacitor currents are, approximately, half the value of the ReSC, due to the fact that each CI-ReSC HB conduct half the current that need to be diverted.

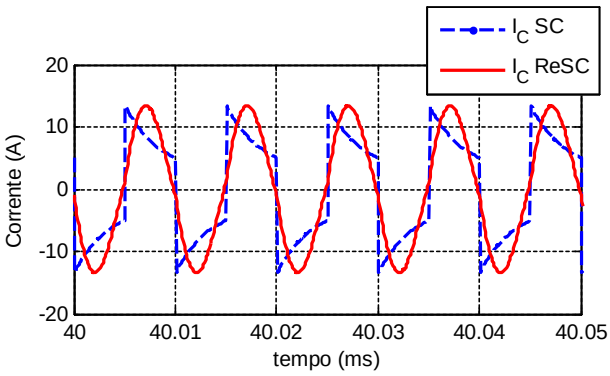

Fig. 9. Capacitor current of both SC and ReSC voltage equalizers.

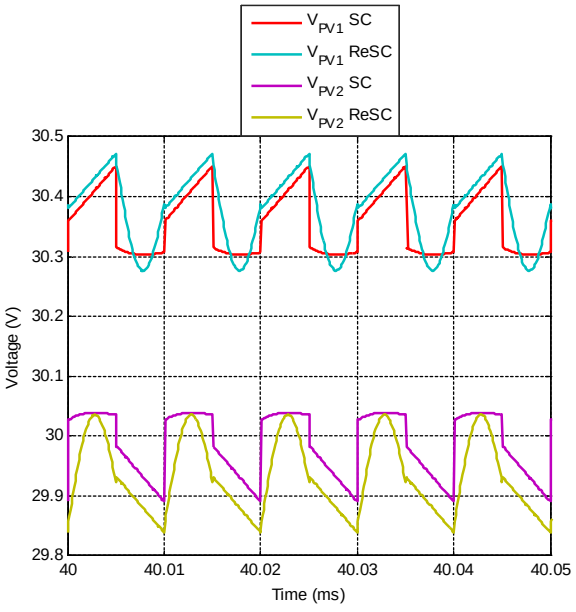

Fig. 10. Module voltages VPV1 and VPV2 for both SC and ReSC voltage equalizers.

For a string with more modules, this circuits are affected by Current Accumulation. A phenomenon detailed in [5], that subject converter in the center level of the string to

higher currents. This is due to current dependency between converters. With the magnetic flux cancellation, the CI-ReSC will be less affected.

It is important to mention that it is possible to use coreless inductors, although more turns will be needed to achieve the inductance, and with the skin effect resultant of high frequency switching, more resistance will be added to the circuit, increasing the EVD.

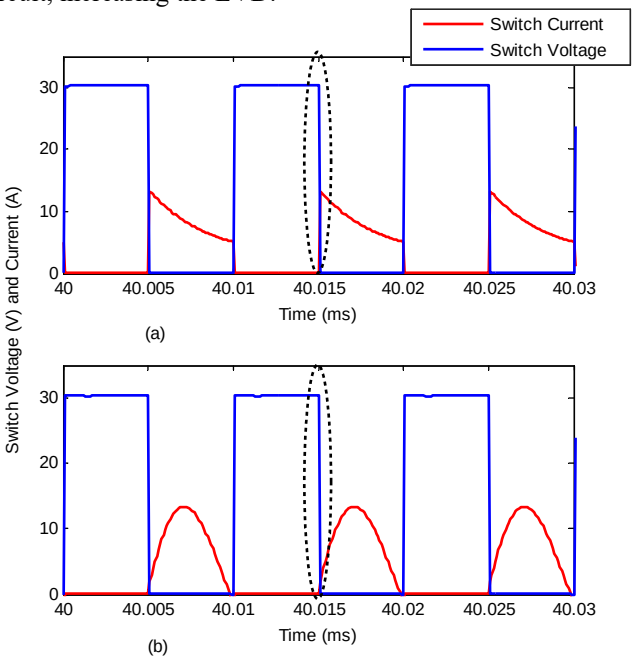

Fig. 11. Switch Current and voltage for both SC and ReSC voltage equalizers.

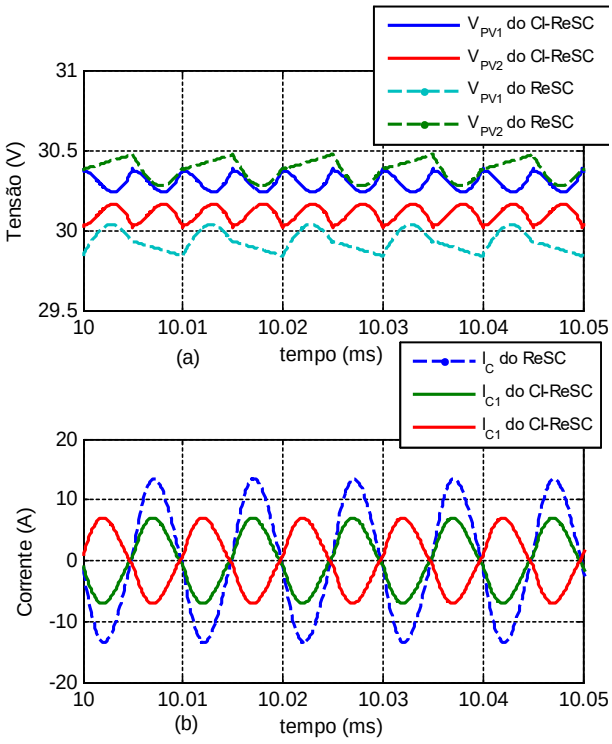

Fig. 12. Comparison between ReSC and CI-ReSC: (a) module voltages; (b) capacitor currents.

VI. EXPERIMENTAL RESULTS

In this section, experimental results of a two module CI-ResC voltage equalizer are shown. In Fig. 13, as can be observed, two 245Wp PV modules are disoriented to emulate module mismatch.

In Fig. 14 pictures of the converter used to implement the CI-ReSC are shown. In Fig. 14 (a), the experiment bench is presented, showing the converters, the capacitors, the measurement instruments, and the resistor used as the modules load. In the picture of Fig. 14 (b), the full-bridges with the LC circuits are shown. As the resonant capacitors C_{x1} and C_{x2}, two 30 µF capacitors are used, connected to a coupled inductor with L_m equal 130 µH, and the L_{x1} and L_{x2} of 1.6 µH. Two 5500 µF capacitor are used to implement C_{d1} and C_{d2} capacitor. The Full-Bridges are implemented with IRF540N MOSFETs, and switched with 10kHz, using an FPGA device to generate the pulses.

Fig. 15 shows the results for voltage equalization using the CI-ReSC. In Fig. 15 (a), as can be observed, before the converter operation, modules voltages are different due to the mismatch, respectively, 20.4V and 30.3V. It means that one module is near the short circuit and the other is near the open circuit. When started, it equalizes the voltages, enabling both modules to operate near the MPP (27.5V), with an EVD of 640mV. This voltage difference, together with the current difference between 5.3A to 3.8A of each module, respectively, indicates an effective resistance of 426 mOhm, in which, the most part comes is the inductor resistance, and approximately, 88 mOhm comes from the MOSFETs R_{on} resistances.

In Fig. 15 (b) the voltage ripple is shown to be considerably small, been affected in most part by stray inductances in the cables.

Fig. 16 shows the resonant capacitors current. As can be noticed, its waveform is similar to a sine wave with RMS values of 544 mA and 538 mA, for each capacitor, which is near the current difference between the mismatched modules. Also, as shown, the switches turns on and off with smaller current values, what reduces switching losses.

Fig. 17 shows a result similar to Fig. 1, in which the load is varied and IxV and PxV are swept. The IxV and PxV curve without voltage equalization indicates two local maxima, while in the equalized there is only one MPP. As expected the MPP of the compensated experiment is considerably higher than the uncompensated. The system with voltage equalizer produces 239.4 Wp while the system without produces only 214.3 Wp.

Although the simulation results shown CI-ReSC advantages compared to ReSC, a consideration of its drawbacks must be considered. The first drawback would be the necessity of another HF, which would increase the converter cost and implementation difficulty. The second drawback, would be the addition of coupled inductors, which implies that ferromagnetic core will be needed. Usually, the tendency is to avoid cores in capacitor switched converter design. However, as mentioned before, the core would require less turns to achieve a proper inductance, resulting in less resistance in the current path for voltage equalization.

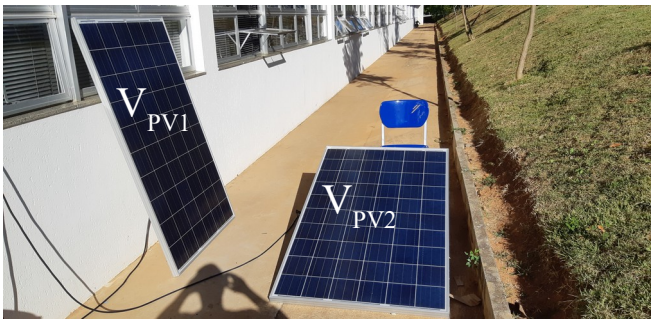

Fig. 13. Picture of mismatched modules.

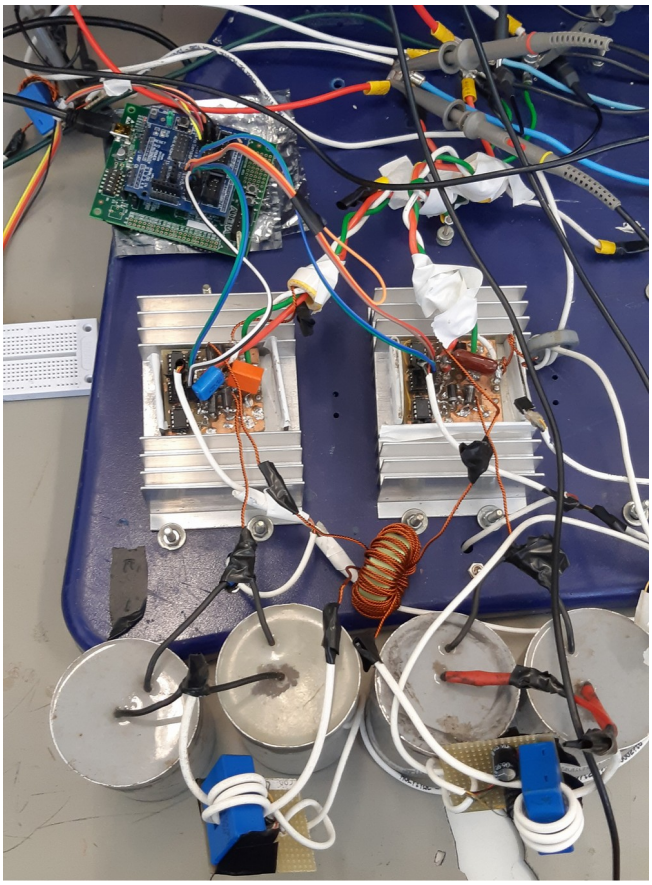

(a)

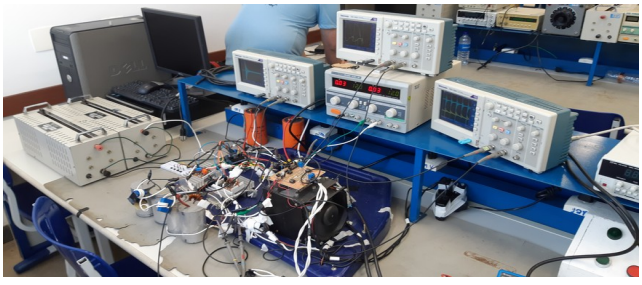

(b)

Fig. 14. Pictures of the experiment bench: (a) Entire experiment bench; (b) Full Bridges with Resonant Capacitors.

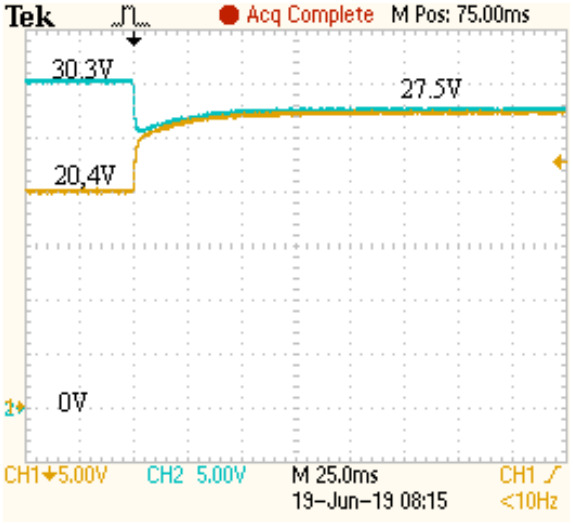

(a)

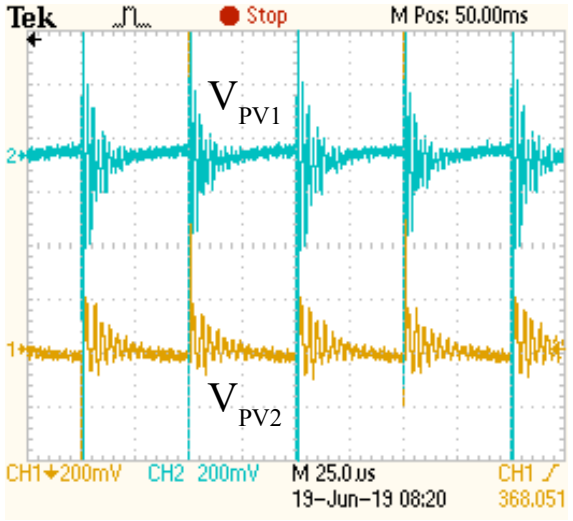

(b)

Fig. 15. Experimental results: (a) Equalized voltages; (b) Equalized voltage ripple.

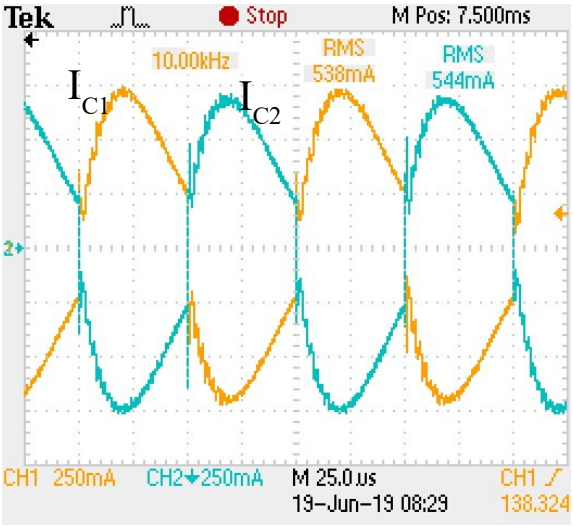

Fig. 16. Experimental results: resonant capacitors currents.

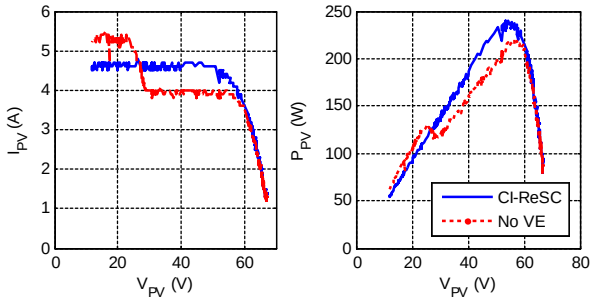

Fig. 17. Experimental results: IxV and PxV for mismatched modules with and without compensation.

VII. CONCLUSIONS

In this paper, a novel voltage equalizer denominated Coupled Inductor Resonant Switched Capacitor is proposed. Switched capacitor converters had played an important role in many power electronics applications, and partial shading compensation is one of them. The SC, as voltage equalizer has shown to be successful, but can be improved with the addition of a inductor, becoming a ReSC. Both have similar performance, but ReSC operates with ZCS and need smaller capacitance on its resonant impedance. The proposed circuit, CI-ReSC, presents lower equalized voltage drop, and reduced levels of current compared with ReSC, as shown by the simulation results. The CI-ReSC circuit was tested experimentally and its results shown that the proposed voltage equalizer operates as expected, enabling the mismatched modules to deliver their total power available. Despite its drawbacks, the proposed circuit shown considerably good performance compared with its predecessor the ReSC, presented half the equalized votlage drop.

REFERENCES

[1] M. Symko-Davies, R. L. Mitchell, C. E. Witt, H. P. Thomas, R. King and D. Ruby, "Decade of PV industry R&D advances in silicon module manufacturing," Conference Record of the Twenty-Eighth IEEE Photovoltaic Specialists Conference - 2000 (Cat. No.00CH37036), Anchorage, AK, USA, 2000, pp. 1460-1463, doi: 10.1109/PVSC.2000.916168.

[2] P. Manganiello, M. Balato, and M. Vitelli, "A Survey on Mismatching and Aging of PV Modules: The Closed Loop," *IEEE Trans. Ind. Electron.*, vol. 62, no. 11, pp. 7276–7286, 2015.

[3] C. Deline, M. Jenya, M. Donovan, and J. Forrest, "Partial Shade Evaluation of Distributed Power Electronics for Photovoltaic Systems," *Photovolt. Spec. Conf. (PVSC), 2012 38th IEEE*, no. June, pp. 1627–1632, 2012.

[4] M. Kasper, D. Bortis, and J. W. Kolar, "Classification and comparative evaluation of PV panel-integrated DC-DC converter concepts," *IEEE Trans. Power Electron.*, vol. 29, no. 5, pp. 2511–2526, 2014.

[5] C. H. G. Santos, P. F. G. Donoso, and S. I. S. Júnior, "Cascaded Cell String Current Diverter For Improvement of Photovoltaic Solar Array Under Partial Shading Problem," *Eletrônica de Potência*, vol. 20, no. 2, 2015.

[6] C. H. G. Santos, P. F. Donoso-garcia, and S. I. S. Junior, "A Comparative Analysis of Voltage Equalizers For Parial Shading Compensation in PV Arrays", *Eletrônica de Potência*, vol. 150, no. V, pp. 100–12, 2019.

[7] K. Kesarwani, R. Sangwan, and J. T. Stauth, "Resonant switched-capacitor converters for chip-scale power delivery: Modeling and design," *2013 IEEE 14th Work. Control Model. Power Electron. COMPEL 2013*, 2013.

[8] A. Blumenfeld, A. Cervera, and M. M. Peretz, "Enhanced differential power processor for PV systems: Resonant switched-capacitor gyrator converter with local MPPT," *IEEE J. Emerg. Sel. Top. Power Electron.*, vol. 2, no. 4, pp. 883–892, 2014.

[9] K. Kesarwani, R. Sangwan, and J. T. Stauth, "A 2-phase resonant switched-capacitor converter delivering 4.3W at 0.6W/mm2 with 85% efficiency," *Dig. Tech. Pap. - IEEE Int. Solid-State Circuits Conf.*, vol. 57, pp. 86–87, 2014.

[10] J. T. Stauth, M. D. Seeman, and K. Kesarwani, "A resonant switched-capacitor ic and embedded system for sub-module photovoltaic power management," *IEEE J. Solid-State Circuits*, vol. 47, no. 12, pp. 3043–3054, 2012.

[11] R. Sangwan, K. Kesarwani, and J. T. Stauth, "High-density power converters for sub-module photovoltaic power management," *2014 IEEE Energy Convers. Congr. Expo. ECCE 2014*, pp. 3279–3286, 2014.

[12] E. Mineiro *et al.*, "Conversor CC / CC Com Capacitor Comutado Aplicado Para Equalização de Potência em Vetores de LEDs", pp. 1100–1108, 2013.

[13] N. Colombo, D. Pont, G. Waltrich, and T. B. Lazzarin, "Transformerless STEP-UP Inverter Based On Switched-Capacitor Converter Technology", no. 1, pp. 269–278, 2017.

[14] C. Julio, T. B. Lazzarin, J. C. Dias, and T. B. Lazzarin, "Retificador Boost Bridgeless Unidirecional Monofásico com Célula de Capacitor Cha-Unidirectional Single-Phase Bridgeless Boost Rectifier with Switched Capacitor", pp. 340–349, 2017.

[15] M. De Andrade, V. Silva, R. De, and T. B. Lazzarin, "Inversor Boost a Capacitor Chaveado Conectado a Rede", pp. 466–476, 2018.

[16] M. A. Salvador *et al.*, "High Gain DC-DC Converter Obtained by Combining Switched Inductor and Switched Capacitor", pp. 161–170, 2018.

[17] R. W. Erickson, *Fundamentals of Power Electronics Fundamentals of Power Electronics*, 2nd ed. New York: Chapman and Hall, May 1997, 2002.

[18] C. H. G. Santos, "Desviadores de Corrente de Arquitetura Híbrida Para Compensação de Sombreamento Parcial em Associações Série de Módulos Fotovoltaicos" UFMG – PPGEE, 2018.

[19] M. Z. Ramli and Z. Salam, "A simple energy recovery scheme to harvest the energy from shaded photovoltaic modules during partial shading," *IEEE Trans. Power Electron.*, vol. 29, no. 12, pp. 6458–6471, 2014.

BIOGRAPHIES

Cláudio H. G. Santos was born in October 05, 1982 in Divinópolis, MG – Brazil. Has received his M.Sc and B.Sc. degrees in Electrical Engineering from CEFET-MG and Doctor in Electrical Engineering from UFMG in Belo Horizonte, Brazil in 2008, 2011 and 2018, respectively.

Nowadays, he is a teacher member of de Mechatronics Engineer Department of CEFET-MG, located in St. Álvares Azevedo 400, in Divinópolis, Brazil. He also had same position in the Federal University of Outo Preto, MG – Brazil. His currently research interest is power-quality-related issues, solar PV technology, switching power supplies and repetitive control. His previous interest was in EMC, antennas and FACTs applications.

Pedro Francisco Donoso-Garcia, has graduated in electrical engineering option in electronics by the Universidade Federal do Rio Grande do Sul – UFRGS in 1981, he received his MSc from the Universidade Federal de Minas Gerais – UFMG and his PhD in Electrical Engineering from the Universidade Federal de Santa Catarina – UFSC in 1986 and 1991 respectively. Currently he is an Associate Professor at the Electronic Engineering Dept.–DELT–UFMG. His research interest include: high efficiency power supply, electronic ballasts and different microgrid aspects, including power electronics and distributed energy-storage systems.

Seleme I. Seleme Jr. was born in Novemeber 03 1955 in Palmas, PR – Brazil. Has graduated in Electrical Engineering from EPUSP at São Paulo in 1977, obtained his M.Sc from UFSC at Florianópolis, in 1985 and his PhD from INPG at Grenoble, France, in 1994. He has made his Post Doctorate at UC Berleley, USA, in 2002. Presently he is an Associate Professor, member of the Electronic Department at the Engineering School, UFMG. His main research interests are power electronics, applied control for static converters, electrical drive systems and electromechanical systems.